

The Relationship between Residual Stresses and Transverse Weld Cracks in Thick Steel Plate

The relationship between longitudinal residual stresses (σ_x direction) and transverse weld cracks was studied for EH32 TMCP 50-mm-thick plate welded with the SAW and FCAW processes

BY H. W. LEE AND S. W. KANG

ABSTRACT. The transverse crack, a type of cold crack, occurs perpendicular to the axis of the weld interface. From experience, longitudinal residual stresses (σ_x direction) are important factors in transverse crack occurrence. Specimens were fabricated and welded under actual construction conditions, then longitudinal residual stresses were measured for different welding conditions using the submerged arc welding (SAW) and flux cored arc welding (FCAW) processes. Transverse weld cracks were detected in specimens welded with preheating and an interpass temperature below 30°C using the FCAW process. Cracks were detected at 9.5–10 mm from the weld face. But in specimens welded with preheating at 70°C, with an interpass temperature below 30°C, and using the SAW process, cracks were detected 9.5–14 mm from the weld face (Refs. 1, 3). The residual stress values for specimens welded at an interpass temperature below 30°C were higher than specimens welded with interpass temperatures of 100–120°C. Also, the residual stress values measured at the weld surface, in the as-welded condition, were higher than longitudinal residual stresses measured from a small test piece due to residual stress relief from the cutting and machining processes. Transverse weld cracks were detected in the area of maximum residual stresses for both the SAW and FCAW processes.

Introduction

Residual stresses are developed in the vicinity of a weld joint during arc welding.

H. W. LEE is with the Welding Research Team of Samsung Heavy Industries, Koje City, Korea. S. W. KANG is with the Research Institute of Mechanical Technology, Busan National University, Korea.

A weldment is locally heated by most welding processes, therefore, the temperature distribution in the weldment is not uniform, and metallurgical changes take place as welding progresses along the weld joint. Therefore, the welding residual stress is sometimes called restraint stress (Refs. 4, 5). These stresses can give rise to distortion and under certain circumstances even to premature failure. Hydrogen-assisted cracking is often detected at a notch in a weld made under restraint. Thus, residual stresses play an important role as far as the quality and reliability of a welded construction are concerned (Refs. 6, 7).

One type of cold crack, referred to as a transverse crack, is caused by a complex interaction of the diffusible hydrogen supply, susceptible microstructure, and tensile residual stress. Previous papers on crack occurrence location, hardness, diffusible hydrogen contents, and microstructure, in accordance with welding conditions, were published in the *Welding Journal* and *Journal of Japan Welding Society* (Refs. 1–3). Hardness in the cracked area (deposited weld metal) was 185–200 HV, and the FCAW and SAW electrodes had diffusible hydrogen contents of approximately 3–7 mL per 100 g of deposited weld metal by the glycerin method.

The weld metal impact test showed

higher absorbed energy for the weld condition with preheating and interpass temperatures at 100–120°C, compared to the specimen welded with preheating and interpass temperatures below 30°C.

Transverse weld cracks were detected in the specimen welded with preheating and interpass temperatures below 30°C with the FCAW process. Cracks were detected 9.5–10 mm from the weld face, between layers 5–8, while in the specimen welded with a preheat of 70°C, interpass temperature below 30°C, and using the SAW process, cracks occurred at 9.5–14 mm from the weld face (Refs. 1–3).

The transverse crack, a type of cold crack, occurs perpendicular to the axis of the weld interface. Therefore, longitudinal residual stresses are more important in transverse cracks.

Until now, few investigations measuring residual stresses in the actual structure have been undertaken. In this study, specimens were fabricated and welded under conditions similar to actual construction conditions, then longitudinal residual stresses were measured for different welding conditions using the SAW and FCAW processes.

Experimental Procedure

Test Weldments: SAW Panel

The test panel was prepared with a double-V groove and welded on two sides using a two-pole submerged arc process. The panel was EH32 TMCP (thermomechanical controlled process), high-strength hull steel (Table 1), to provide test conditions similar to actual construction conditions. To magnify fabrication-related weld residual stresses, the test panel was restrained by a jig, as shown in Fig. 1.

The size of the test panel was 10 m (32.8 ft) long \times 3.6 m (11.8 ft) wide \times 50 mm (2

KEY WORDS

Residual Stresses
Transverse Weld Cracks
Preheat
Interpass Temperatures
Flux Cored Arc Welding (FCAW)
Submerged Arc Welding (SAW)

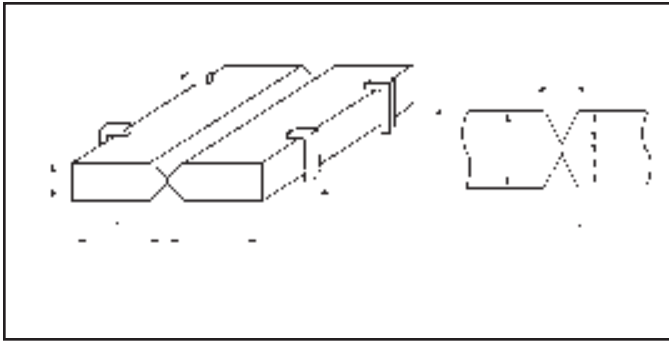


Fig. 1 — Schematic diagram of weld panel for the SAW process.

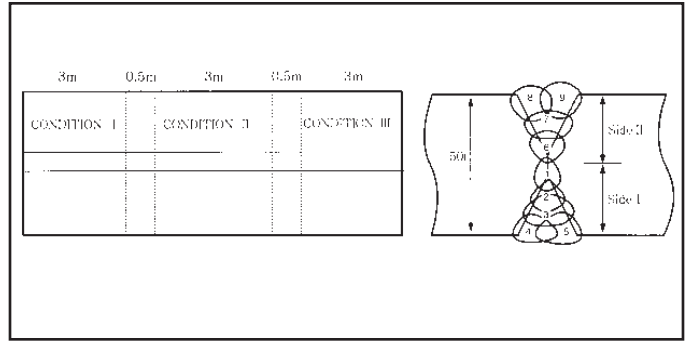


Fig. 2 — Schematic diagram of the weld deposit metal for the SAW process.

Table 1 — Chemical Composition of Base/Weld Metal for the SAW Process

(%)	C	Si	Mn	P	S	Ni	Mo	V	Ti	T.S. (N/mm ²)	Y.S. (N/mm ²)	EL (%)
EH32 TMCP	0.18 max.	0.10 ~ 0.50	0.90 ~ 1.60	0.040 max.	0.040 max.	0.040 max.	0.08 max.	0.10 max.	0.02 max.	440 ~ 590	310 min.	20.0 min.
Base Metal	0.10	0.35	1.48	0.018	0.006	0.03	0.02	0.001	0.02	523	395	30.5
Weld Metal A	0.09	0.32	1.33	0.025	0.013	0.03	0.05	0.003	0.01	553	442	28.5
Weld Metal B	0.09	0.30	1.33	0.025	0.013	0.03	0.06	0.003	0.01	597	487	25.3

A: preheating 70°C, interpass temp. below 30°C (10 mm from weld face of side I).
 B: preheating 70°C, interpass temp. 100 ~ 120°C (10 mm from weld face of side II).

Table 2 — Welding Parameters for SAW Process

Pass No.	Current (A)		Voltage (V)		Welding Speed (cm/min)	Heat Input (kJ/cm)			
	Lead (DCEP)	Trail (AC)	Lead	Trail		Lead	Trail	Total	
Side I	1	600	820	35	40	100	12.6	19.6	32.2
	2	900	820	35	40	82	23.0	24.0	47.0
	3	920	900	34	40	60	31.2	36.0	67.2
	4	920	900	34	40	90	20.8	24.0	44.8
	5	980	900	34	38	90	22.2	22.8	45.0
Side II	6	1200	800	35	44	70	36.0	30.1	66.1
	7	1000	900	35	38	60	35.0	34.2	69.2
	8	1000	900	34	38	70	29.1	29.3	58.4
	9	1000	900	34	38	70	29.1	29.3	58.4

Table 3 — Preheating and Interpass Temperature for the SAW Process

Condition	Preheating Temperature	Interpass Temperature	
		Side I	Side II
Condition I	70°C	100 ~ 120°C	100 ~ 120°C
Condition II	70°C	100 ~ 120°C	below 30°C
Condition III	70°C	below 30°C	below 30°C

in.) thick, as shown in Fig. 1. The panels were welded using AWS A5.17/F7AZ-EH14 electrode/flux combination with the SAW process using a tandem arc (4.8-mm-diameter electrodes with an extension of 25–30 mm).

The sections were welded under the following conditions: 1) *A* was welded with 70°C preheat (158°F) and interpass tem-

peratures of 100~120°C (212~248°F); 2) *B* was welded with 70°C preheat and an interpass temperature below 30°C (86°F).

The panel was welded in three parts (welding was interrupted at a 0.5-m width between welding conditions) with different interpass temperatures, as shown in Fig. 2. Welding parameters are shown in Tables 2 and 3.

FCAW Panel

The size of the test panel was 2 m (6.6 ft) long < 1.8 m (5.9 ft) wide < 50 mm (2 in.) thick. These test conditions were similar to actual construction conditions — Fig. 3. To magnify fabrication-related weld residual stresses, the welding jig and test panel were fillet-welded together.

Two sets of test panels were made the same size and morphology, as shown in Fig. 3. The specimen sections were welded in layers, as shown in Fig. 4. To compare the residual stresses and the places of transverse crack occurrence, the sections were welded under the following conditions: 1) One was welded below 30°C for preheating and interpass temperatures; 2) the other was welded with preheating and

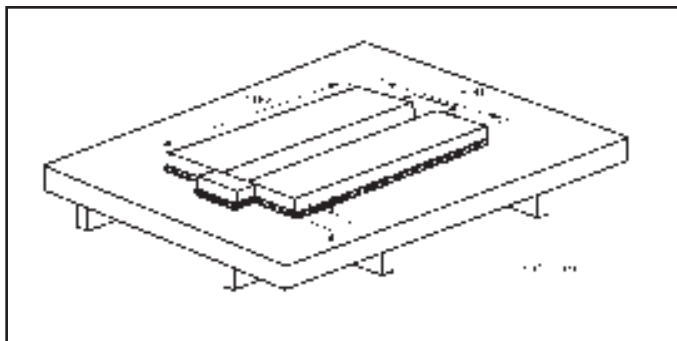


Fig. 3 — Schematic diagram of weld panel for the FCAW process.

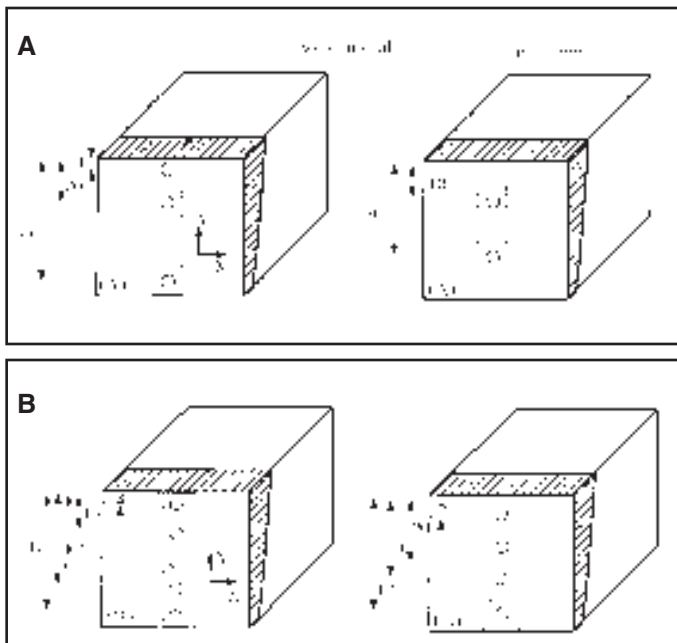


Fig. 5 — The position of attached Rosette gauge for residual stress measurement of the cutting method. A — FCAW process; B — SAW process.

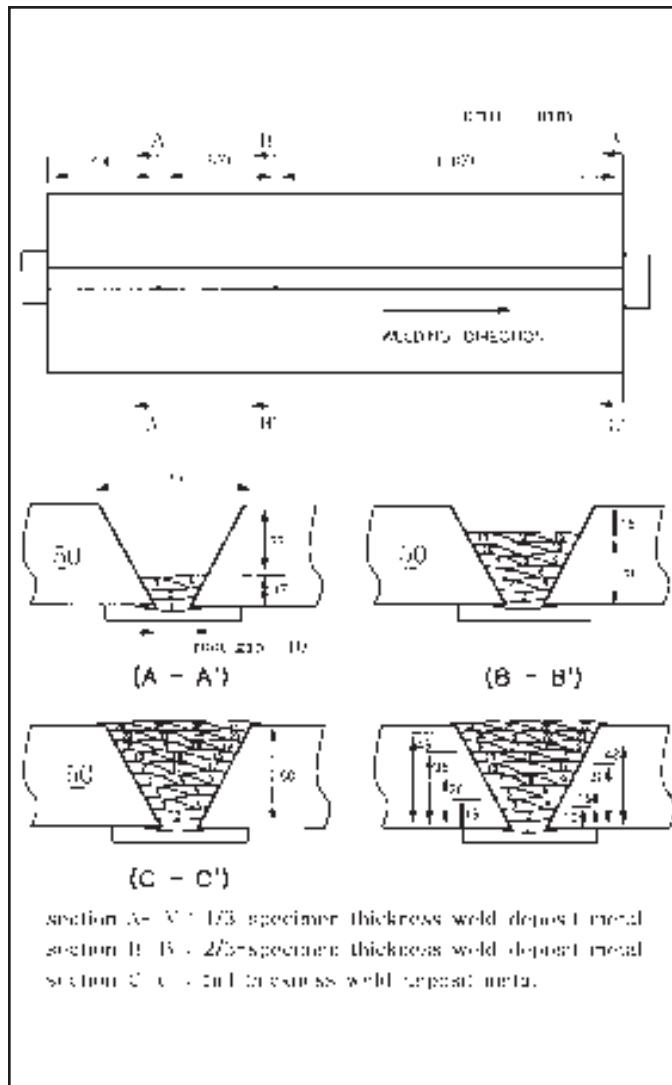


Fig. 4 — Schematic diagram of weld deposit metal for the FCAW process. A-A' — $\frac{1}{3}$ -thickness of deposited weld metal; B-B' — $\frac{2}{3}$ -thickness of deposited weld metal; C-C' — full thickness of weld deposit.

Table 4 — Welding Parameters for the FCAW Process

Identification	Welding Condition	Pass	Current (A)	Voltage (V)	Speed (cm/min)	Heat Input (kJ/cm)
A	preheating/interpass temperature below 30°C	1	240 ~ 250	30	16	28
		2 ~ 27	340 ~ 350	35	37 ~ 41	19
B	preheating/interpass temperature 100 ~ 120°C	1	240 ~ 250	30	15	29
		2 ~ 27	340 ~ 350	35	38 ~ 42	18

interpass temperatures of 100–120°C (212–248°F).

The preheating temperature of 100°C was obtained with the Yurioka method (Ref. 8) (Table 4, 50-mm-thick steel plate, C_{eq} 0.34). The test specimens were welded at 100–120°C in consideration of ambient

temperatures. The panel was welded with AWS A5.29 E81T1-K2 electrodes, using the flux cored arc welding process (1.2 mm diameter, 20 L/min flow rate, 100% CO₂ gas, semiautomatic, electrode extension 25–30 mm). Welding parameters are shown in Table 4.

Chemical Composition/Strength

A spectroanalyzer (Baird Spectrovac-2000, USA) was used to determine the chemical composition of the base and weld metal. Mean values of the three specimens were then recorded in Tables 1 and 5, respectively.

Strength was measured using a universal testing machine (Shimadzu UH-F100A, Japan). Tensile test specimens were made from all deposited metal in a direction parallel to the welding direction. The specimens were the round-bar type, taken 10 mm from the weld face, and recorded in Tables 1 and 5, respectively. Other test results such as hardness, microstructure, residual stresses, absorbed energy, diffusible hydrogen contents, and crack position were published in previous papers (Refs. 1–3).

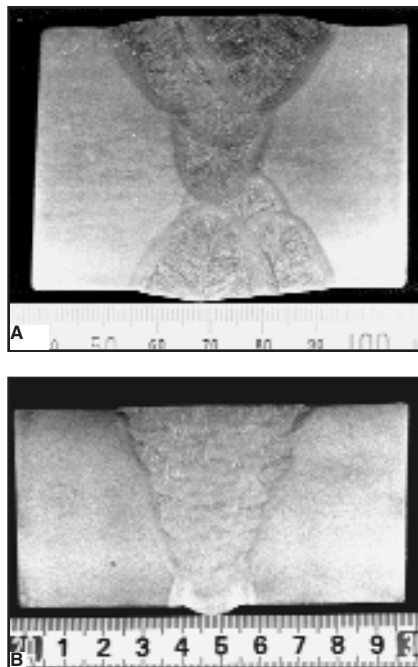


Fig. 6 — Macrostructure of weldments. A — SAW process; B — FCAW process.

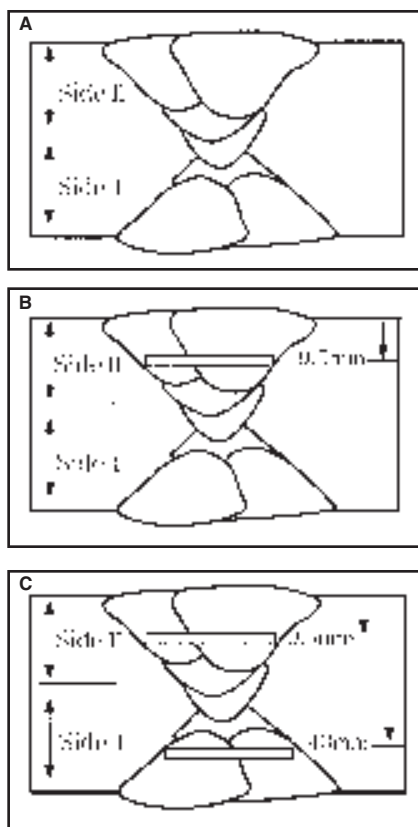


Fig. 7 — The transverse crack position according to changing welding conditions with the SAW process. A — Preheat 70°C, interpass temp. 100~120°C both side 1 and side 2; B — preheat 70°C, interpass temp. 100~120°C (side 1), below 30°C (side 2); C — preheat 70°C, interpass temp. below 30°C both side 1 and side 2.

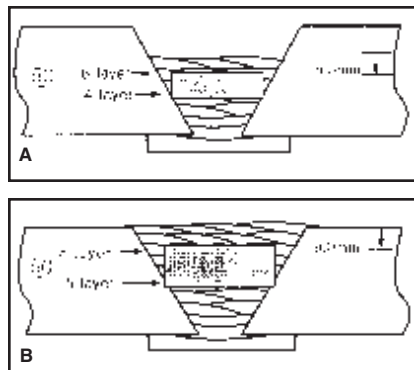


Fig. 8 — The transverse crack position according to changing welding conditions with the FCAW process. A — 35-mm weld joint; B — 50-mm weld joint.

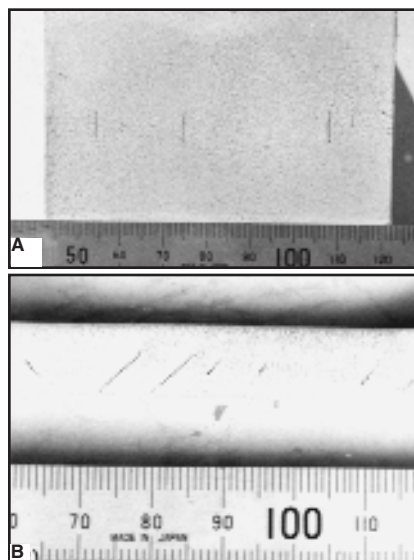


Fig. 9 — Morphology of transverse cracks after magnetic particle inspection for FCAW process. A — 9.5mm depth from the weld face; B — longitudinal section perpendicular to the plane of the plate.

Distinction of Crack Position

To check the position and length of the transverse cracks according to changing layer and preheating and interpass temperatures, the specimens were inspected by ultrasonic testing. The face of the weld bead was then cut at 0.5-mm-depth intervals using a milling machine and checked for accurate position and length of the transverse cracks using magnetic particle inspection after each machining step.

Residual Stresses

The residual stresses were measured using the Rosette gauge, hole-drilling method, per ASTM E837-01 (Ref. 9). The surface residual stresses of FCAW along the weld metal centerline (σ_x direction) were measured in the as-welded condition after the specimen cooled completely.

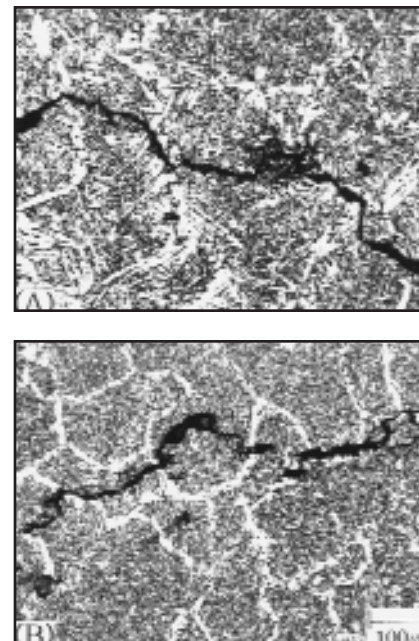


Fig. 10 — Optical micrographs of the transverse crack area taken from Fig. 9A.

To measure the longitudinal residual stresses as a function of depth in the joint, the specimens were machined to expose the longitudinal centerline, as shown in Fig. 5. The specimens were taken from the center of the test panel.

Longitudinal residual stresses were measured for both the SAW and FCAW processes. In the specimen welded with SAW, the Rosette gauges were attached 3, 8, 15, 20, 25, 30, 35, 42, and 47 mm from the weld face. The specimens welded with the FCAW process had the Rosette gauges attached 3, 10, 20, 30, and 45 mm from the weld face.

Results and Discussion

Macrostructure

Figure 6A and B shows the macrostructure of SAW and FCAW, respectively. The Fig. 6A panel was welded with preheating and interpass temperatures below 30°C, and 6B panels were welded with preheating at 70°C and interpass below 30°C.

Position and Morphology of Crack

Figure 7 shows the positions of transverse weld cracks for the SAW process. Transverse cracks were detected in the specimen welded with a preheat of 70°C and an interpass temperature below 30°C, as shown in Fig. 7. Cracks were not detected for the specimen welded with 70°C preheating and interpass temperatures of 100~120°C. The cracks were detected 9.5–14 mm from the weld face.

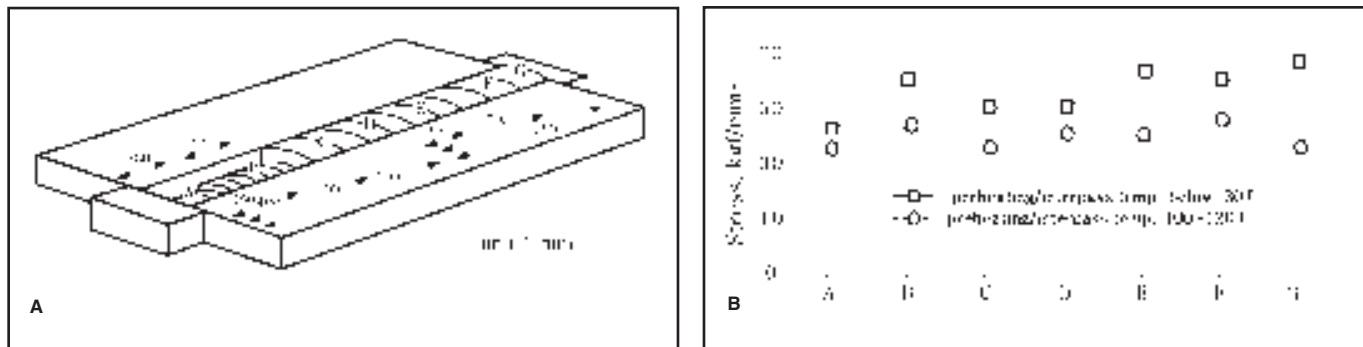


Fig. 11 — Surface residual stress of longitudinal direction in deposited metal with FCAW process. A — position of attached Rosette gauge; B — distributions of surface residual stresses.

Table 5 — Chemical Composition of Base/Weld Metal for the FCAW Process

(%)	C	Si	Mn	P	S	Ni	Mo	V	Ti	T.S. (N/mm ²)	Y.S. (N/mm ²)	EL (%)
EH32 TMCP	0.18 max.	0.10 ~ 0.50	0.90 ~ 1.60	0.040 max.	0.040 max.	0.040 max.	0.08 max.	0.10 max.	0.02 max.	440 ~ 590	310 min.	20.0 min.
Base Metal	0.09	0.38	1.35	0.015	0.005	0.03	0.02	0.002	0.02	517	372	31.0
Weld Metal A	0.04	0.29	1.05	0.012	0.017	1.32	0.02	0.017	0.01	680	624	22.8
Weld Metal B	0.04	0.29	1.03	0.013	0.016	1.31	0.02	0.018	0.01	650	602	23.4

A: preheating and interpass temperature below 30°C (10 mm from weld face).

B: preheating and interpass temperature 100~120°C (10 mm from weld face).

Figure 8 shows the positions of transverse weld cracks for the FCAW process. Transverse cracks were detected in the specimen welded with preheating and interpass temperatures below 30°C, but cracks were not detected for the specimen welded with preheating and interpass temperatures of 100~120°C. The cracks were detected at 9.5~10 mm from the weld face.

Figure 9 shows the morphology of transverse cracks for FCAW after magnetic particle inspection. Figure 9A shows the morphology of a crack at a 9.5 mm depth from the weld face. The cracks oriented perpendicularly to the welding axis.

Figure 9B shows a longitudinal section perpendicular to the plane of the plates. The cracks were observed 45 deg to the longitudinal section, perpendicular to the plane of the plates. These cracks are called chevron cracks, transverse 45-deg cracking, or staircase cracking. Chevron cracking is the most used. The cracks are characterized by their orientation, which is approximately transverse to the welding direction and at 45 deg to the plane of the plate in a butt joint (Refs. 10, 11).

Figure 10A and B shows an optical micrograph of the transverse crack area. The formation of these cracks did not follow the grain boundary ferrite, rather, they propagated across the grains. From fracture morphology, it is noted that transverse cracks occur in high stresses.

Residual Stresses

Figure 11 shows the longitudinal surface residual stresses for FCAW. The residual stresses were measured at the surface of the deposited metal in a longitudinal direction to the weld interface. In all measured points, the residual stress values for specimens welded with preheating and interpass temperatures below 30°C were higher than those welded with preheating and interpass temperatures of 100~120°C.

Figure 12 shows the residual stresses of longitudinal stresses as a function of depth in the joint for SAW. The residual stresses were measured in the longitudinal direction of the deposited metal. For most of the measured points, the residual stress values for a specimen welded with 70°C preheating and interpass temperatures below 30°C were higher than for specimens preheated at 70°C and with interpass temperatures of 100~120°C. For the same method, residual stresses measured in the longitudinal direction of the deposited metal for FCAW are shown in Fig. 13. For most of measured points, the residual stress values for a specimen welded with preheating and interpass temperatures below 30°C were higher than the specimens with preheating and interpass temperatures of 100~120°C. Slightly higher residual stresses were measured in welds

with lower preheat and interpass temperatures, but the deviation of residual stresses measured for as-welded conditions may be higher than that of residual stresses measured in a small machined test piece.

The residual stress values for a specimen measured at the weld surface, in the as-welded condition, were higher than longitudinal residual stresses that were measured from a small test piece at the same position. The residual stress values were about five times higher as shown in Figs. 11 and 13. This was because the residual stress was relieved during the machining process, before residual stress measurement.

The tendency of residual stress agreed with other research (Refs. 12, 13). In multipass welds, residual stress is distributed nonuniformly.

Gunnert (Ref. 12) has shown the directions of residual stress distribution in low-carbon steel weld metal in a 1-in. (25 mm)-thick butt joint. Welding was sequenced alternately on both sides to minimize angular distortion. High longitudinal tensile residual stresses were found in the areas near the surface of the weld.

Transverse cracks were detected in area of the maximum residual stress for both the SAW and FCAW processes. The residual stresses and hydrogen accumulation may be at a maximum in those loca-

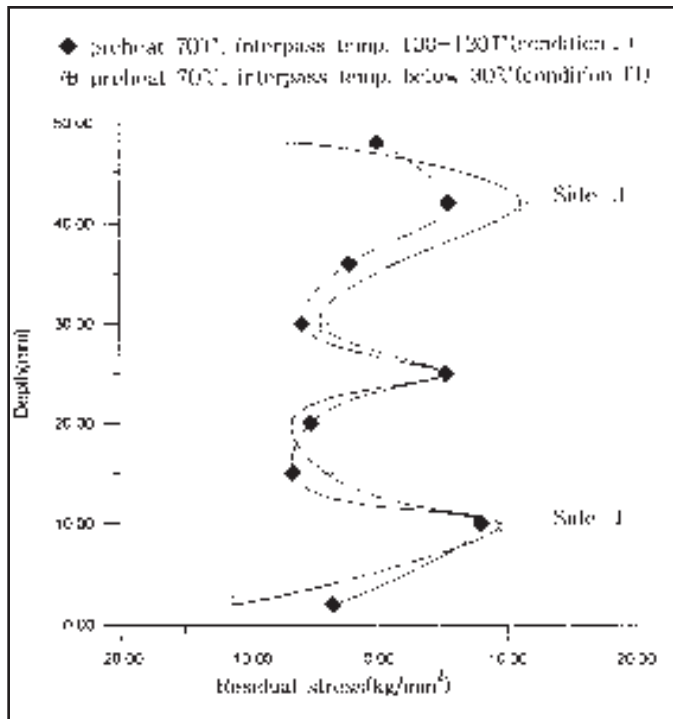


Fig. 12 — Distributions of longitudinal residual stress as a function of depth in the joint for SAW process.

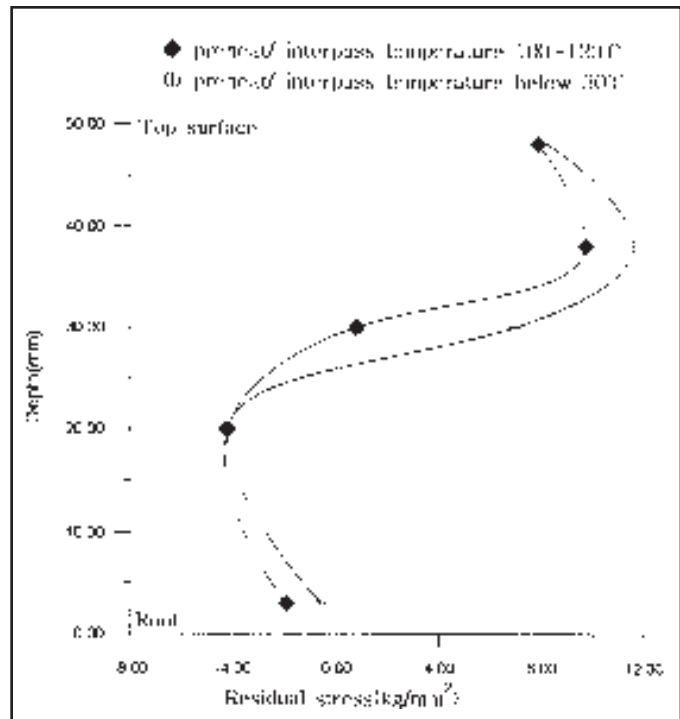


Fig. 13 — Distributions of longitudinal residual stress as a function of depth in the joint for the FCAW process.

tions (Ref. 14). It is believed they directly affected transverse crack occurrence.

Conclusions

The relationship for residual stresses, longitudinal stresses, and transverse weld cracks was studied for EH32 TMCP 50-mm-thick plate welded with the SAW and FCAW processes. The results of this study can be summarized as follows:

1) Transverse weld cracks were detected in the specimen welded with preheating and interpass temperatures below 30°C with the FCAW process. The cracks were detected 9.5–10 mm from the weld face.

In the specimen welded with 70°C preheating and an interpass temperature below 30°C using the SAW process, cracks were detected 9.5–14 mm from the weld face.

2) The formation of transverse weld cracks did not follow the grain boundary ferrite, rather, they propagated across the grains. From fracture morphology, it is noted that transverse cracks occur in high stress areas.

3) The residual stress values for a specimen measured at the weld surface, in the as-welded condition, was higher than that of longitudinal residual stresses measured from a small test piece due to the relief of residual stresses by the cutting and machining processes.

4) The residual stress values for the

specimen welded with an interpass temperature below 30°C was higher than the specimen welded at interpass temperatures of 100–120°C. Transverse weld cracks were detected in the area of the maximum residual stresses for both the SAW and FCAW processes.

References

1. Lee, H. W., Kang, S. W., and Um, D. S. 1998. A study on transverse weld cracks in thick steel plate with the FCAW process. *Welding Journal* 77(12): 503-s to 510-s.
2. Lee, H. W., Kang, S. W., and Park, J. U. 2001. Fatigue strength depending on position of transverse cracks in FCAW process. *Welding Journal* 80(6): 137-s to 141-s.
3. Lee, H. W., and Kang, S. W. 1997. A study on transverse weld cracks in 50-mm-thick steel plate with the SAW process. *Journal of Japan Welding Society* 15(4): 563–573.
4. Kou, S. 1987. *Welding Metallurgy*. New York, N.Y.: John Wiley and Sons, pp. 109–113.
5. Brand, P. C., De Keijser, Th. H., and Den Ouden, G. 1993. *Welding Journal* 72(3): 93-s to 100-s.
6. Yurioka, N., and Suzuki, H. 1990. Hydrogen assisted cracking in C-Mn and low alloy steel weldments. *International Materials Reviews* 35(4): 217–245.
7. Hart, P. H. M. 1986. Resistance to hydrogen cracking in steel weld metals. *Welding Journal* 65(1): 14-s to 22-s.
8. Yurioka, N. 1995. A chart method to determine necessary preheat temperature in steel welding. *Journal of Japan Welding Society*, pp. 347–350.
9. ASTM. 1997. Test Method E837-01.

Standard Test Method for Determining Residual Stresses by the Hole-Drilling Strain-Gauge Method.

10. Mota, J. M. F., and Apps, R. L. 1982. Chevron cracking — a new form of hydrogen cracking in steel weld metals. *Welding Journal* 61(7): 222-s to 228-s.

11. Allen, D. J., Chew, B., and Harris, P. 1982. The formation of chevron cracks in submerged arc weld metal. *Welding Journal* 61(7): 212-s to 221-s.

12. *Welding Handbook*, 8th ed., Vol. 1. Welding technology. Miami, Fla.: American Welding Society, pp. 109–113, 238–241.

13. Shim, Y., Feng, Z., Lee, S., Ki, D., and Jaeger, J. C. 1992. Determination of residual stresses in thick-section weldments. *Welding Journal* 71(9): 305-s to 312-s.

14. Takahashi, E. 1979. Relations between occurrence of the transverse cracks. *Journal of Japan Welding Society*, pp. 855–872.

REPRINTS REPRINTS

To order custom reprints of articles in
Welding Journal,
contact Denis Mulligan at
(800) 259-0470
FAX: (717) 481-7677
or via e-mail at
info@reprintdept.com

REPRINTS REPRINTS